Assimilation of water vapour radiances from geostationary imagers and HIRS at ECMWF

Christina Köpken, Graeme Kelly, Jean-Noël Thépaut

ECMWF, Shinfield Park, Reading
RG2 9AX, United Kingdom
Christina.Koepken@ecmwf.int

ABSTRACT

This paper describes the direct assimilation of water vapour radiances at ECMWF, the emphasis being put on the usage of the clear-sky water vapour radiances from geostationary satellites, which became operational in April 2002 using data from Meteosat–7. Currently, experiments are being carried out to extend the coverage by geostationary radinaces using data from the GOES satellites. As the four–dimensional variational assimilation includes the time dimension, the high temporal resolution of the geostationary radiance data can be exploited to provide information not only on the upper tropospheric humidity but also on the upper tropospheric wind field. Extensive pre-operational monitoring of the geostationary clear–sky radiance data has been carried out. It shows a systematic warm bias of approximately 2–3 K for the Meteosat water vapour radiances compared to the model first guess fields, while the bias of water vapour radiances from the GOES satellites and both HIRS and AMSUB with respect to the first guess remain within about $\pm$1–1.5 K. Additionally, the monitoring shows regular image and radiance anomalies for the geostationary satellites. When assimilated the geostationary radiances correct the upper tropospheric humidity field in areas of known model problems. While the analysis draws well to the data, the fit to other conventional observations does not degrade, and the fit to other satellite observations is noticeably improved. The impact on forecast quality is slightly positive to neutral for different areas of the globe with a positive impact being noted in the upper level wind fields and geopotential. The introduction of data from additional HIRS channels likewise improves forecast quality. The influence of a new humidity analysis variable on increment structures and background errors for radiance assimilation is also briefly discussed.

1 Introduction

For a global analysis, the upper tropospheric humdity field can only insufficiently be constrained by conventional observations since measurements are scarce over large regions of the globe and, additionally, radiosondes usually display larger errors under extremely cold conditions of high altitudes. In the ECMWF analysis radiosonde data are therefore only used up to a level of 300 hPa. Satellite observations play thus an important role for analysing the upper tropospheric humidity. This paper describes the assimilation of water vapour (WV) radiances at ECMWF, concentrating particularly on the recent developments on the usage of data from geostationary satellites which became operational on 9 April 2002 using data from Meteosat–7. While the direct assimilation of radiances from sounding instruments on polar orbiting satellites is well established for numerical weather prediction (NWP) (e.g. Andersson et al., 1994; McNally et al., 2000), data from geostationary imagers have primarily been used either in the form of atmospheric motion vectors (AMV) derived from tracking features in the imagery or in the form of cloud top information (e.g. MacPherson et al., 1996). Compared to radiance observations from polar orbiting satellites, data from geostationary platforms offer a considerably higher time resolution and therefore a quasi–continuous description of the water vapour field in the high troposphere. Within 4DVAR (see e.g. Rabier et al., 1998) it is possible to take advantage of this high temporal resolution which provides not only information about the time evolution of the UTH field but also about the wind field, so that analysis increments can be derived for both humidity and wind fields.
This paper describes in the Section 2 the data used together with quality control issues for both HIRS and geostationary data. Section 3 concentrates on analysis changes due to the usage of geostationary radiances, while

verification and forecast impact are discussed in Section 4. Section 5 invstigates further the vertical structure of analysis increments and changes caused by the new formulation of humidity analysis which is currently being developed and described in a paper by Holm et al. (this issue). A summary is given in Section 6.

2 Data and data usage

The data currently used for operational analyses are the channel 12 of the High-Resolution Sounder (HIRS) on board the polar orbiting NOAA satellites and the water vapour channel of the geostationary satellite Meteosat–7. The usage of additional WV radiances is currently being tested in pre–operational trials. These include the humidity channel HIRS 11 (along with channels 4–7, 14, 15) and the WV channels of the two operational GOES satellites GOES–8 and GOES–10. Meteosat–5 data are not yet currently used since the vicarious calibration (van de Berg et al., 1995), which is not stable enough for assimilation purposes, has only been replaced in mid 2001 by the more stable cross–calibration versus Meteosat–7 (using the overlap area between the two satellites). Before usage, these data needed further monitoring, particularly also during eclipse periods. Some remaining problems visible in the radiance monitoring are currently being solved by EUMETSAT which should enable future quantitative usage for assimilation.

2.1 Geostationary clear–sky radiances

The raw radiances from geostationary platforms represent a huge data volume due to their high horizontal resolution. Furthermore, the assimilation of radiances affected by clouds currently presents difficulties due to uncertainties in the model cloud parameters, their interaction with radiation transfer and limitations in the accuracy of the tangent linear and adjoint models of 4DVAR. Therefore, the geostationary WV radiances are pre-processed to area averages of clear–sky radiances (CSR). For Meteosat–5 and –7 the CSR (processed by EUMETSAT) have about 80x80 km^2 resolution at Sub-Satellite Point (SSP). Those from the GOES satellites (processed since November 2001 by the Cooperative Institute for Meteorological Satellite Studies, CIMSS, USA) have about 40x40 km^2 at SSP. This resolution compares more favourably with the resolution of the anaylsis increments (about 125 km) than that of the raw data which should improve the representativity of the observations. CSR data from both the Meteosat and GOES satellites are available at hourly time resolution.

2.2 Cloud detection for HIRS

For cloud detection in the HIRS channels, a new scheme has been implemented which follows ideas developed for the cloud detection from data of the Atmospheric Infrared Sounder (AIRS), see McNally and Watts (2002). The channels are ranked according to the altitude of the peak of their weighting functions and then first guess departures are checked starting with the stratospheric channels which are not affected by cloud and continuing for consecutively lower peaking channels. When a channel is cloud contaminated, this and the lower peaking channels will have a noticeably more negative first guess departure. While the previously used window channel check relies on a well known lower boundary condition (i.e. surface temperature), this check needs a good first guess of stratospheric temperatures. The model's stratospheric temperatures have been shown to be of sufficiently good quality due to the availability and use of data from the Advanced Microwave Sounding Unit (AMSU). Advantages of the scheme are, that the cloud detection works much more reliably also over land and that in case of clouds being detected in a certain channel, the higher peaking channels can still be assimilated.

2.3 Quality issues for geostationary CSR

Detailed monitoring of geostationary CSR has shown a number of issues which need to be taken into account before assimilating the data. First, since the analysis method assumes unbiased observation and first guess values, it has to be ensured that the data are free of biases. Figure 1 compares the hourly brightness temperature (TB) observations from Meteosat and GOES satellites as well as HIRS–12 and AMSUB–3 on NOAA to the corresponding model first guess, i.e. the brightness temperature computed using RTTOV–6M (Matricardi et al., 2001) and the model temperature and humidity profiles. Relative to the model, HIRS–12 and AMSUB–3

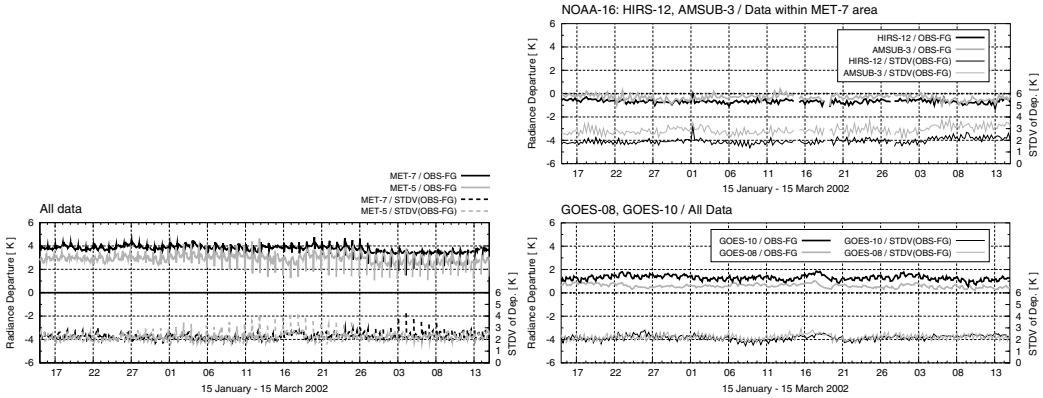

Figure 1: Time series of mean differences between radiance observations and model first guess (as brightness temperatures in K, left axis) and standard deviations of the differences (right axis) for 15 January 2002 until 15 March 2002. Left panel: For Meteosat–7 (black curves) and Meteosat–5 (grey curves) CSR. Top right panel: For NOAA–16 HIRS–12 (black curve) and AMSUB–3 (grey curve) data within a square area covering the Meteosat–7 disk. Bottom right panel: For GOES–08 (grey curve) and GOES–10 (black curve) CSR.

have relatively small mean biases of about -0.7 K and -0.3 K, respectively (results of other NOAA satellites being similar). GOES–10 and GOES–8 CSR have 1.5 K and 0.8 K positive bias, respectively, while Meteosat–7 (5) TB are on average considerably warmer having about 3.8 K (3 K) bias. Although verification of RTTOV shows that RTTOV contributes approximately 0.7 K to this bias, the radiances from Meteosat seem biased high compared to the model and the other satellites. The standard deviations of departures of the different radiances are all comparable at about 2 K. In order to correct for the biases and also to bring the different instruments in accordance with each other, all radiances are bias corrected using the analysis around radiosonde stations as a reference. The bias correction is a statistical regression using model predictors, the coefficients of the multivariate regression being derived from bout 3–4 weeks of statistics of observation minus analysis departures. For NOAA data, additionally a scan correction is applied, while for the geostationary data, no dependence of the bias on scan position (or viewing angle) was found.
Figure 1 indicates also other effects that concern specifically the geostationary data: Time series of observation minus first guess values for Meteosat data show charateristic spikes for data around local midnight which are particularly big during eclipse periods. The effects are caused by solar stray light entering the radiometer and creating different anomaly patterns like warm bows, small very intense warm spots, warm and cold horizontal stripes and too cold calibration of large parts of certain images. Such effects of stray light were known at EUMETSAT since the early years of the Meteosat programme and efforts have always been made to diminish the impact by not producing products from such Meteosat image data. However, a detailed study based on the ECMWF monitoring shows that the effect is discernable in radiance products for periods much longer than those considered in the operational system (Köpken, 2002; Köpken, 2001). The periods for which data may be affected and are therefore excluded from assimilation are summarized in Table 1.

Also the GOES radiances seem to display a 'midnight effect' consisting of an anomalously cold calibration as suggested by the diurnally occuring lower biases in Figure 1. Effects seem stronger for GOES–8 and are possibly caused by a general heating of the satellite by the sun. Parts of the satellite radiate back onto the

Table 1: Periods during which some contamination of Meteosat–7 or Meteosat–5 CSR is diagnosed from the ECMWF monitoring. Based on data during from April 2000 through to May 2002. (Periods are chosen as to rather flag too many than too few images).

	Anomalies Diagnosed in Monitoring	
CSR slot	Spring Eclipse	Autumn Eclipse
Meteosat–7		
23 UTC	08/03 – 13/04	27/08 – 20/10
00 UTC	15/02 – 21/05	24/07 – 22/12
01 UTC	throughout the year	throughout the year
02 UTC	20/01 – 21/05	26/07 – 08/11
03 UTC	26/01 – 20/04	27/08 – 28/10
Meteosat–5		
20 UTC	20/01 – 12/05	10/07 – 10/11
21 UTC	throughout the year	throughout the year
22 UTC	20/01 – 21/05	10/08 – 20/10

black body, which (being not an ideal black body) reflects a very small portion back leading to an erroneous calibration reading (Johnson and Weinreb, 1996). Therefore, data close to local midnight from GOES–8 and GOES–10 are currently excluded all year round (images of 2–8 UTC (7–10 UTC) for GOES–8 (GOES–10)) as a precaution until the exact extent of anomalies can be better determined.
Last, although the geostationary radiances are clear–sky, there is an indication of remaining cloud contamination. Based on image overlays and histograms of first guess departures, additional quality check criteria have been introduced. Observations with a low percentage of clear pixels contributing to the CSR mean or anomalously cold departures in the IR window channel are excluded. Also during thinning, observations with a high percentage of clear pixels and warmer IR temperatures are given preference (see Köpken et al., 2002). Additionally, all data have to pass a first guess check and a variational quality control check (Andersson and Järvinen, 1999). CSR data are used at the hourly time resolution. Horizontally, both the CSR and the HIRS data are thinned to 1.25°.

3 Influence of geostationary WV radiances on the model fields

Several assimilation experiments have been conducted using Meteosat–7 and more recently GOES–8 and GOES–10 CSR data in the 4DVAR in addition to all other operationally used observations, including especially HIRS–12 radiances and AMVs from Meteosat, GOES and GMS satellites. Figure 2 shows in the top panel the mean change in upper tropospheric humidity (here relative humidity at 300 hPa) due to the assimuilation of WV CSR from GOES. Within the area covered by GOES–8 nd –10 there is characteristically a decrease of upper level humidity in the convective areas of the Inner Tropical Convergence Zone (ITCZ) and the Southern Pacific Convergence Zone (SPCZ) while humidity is increased in adjacent areas (changes being about 2-10 %). The scattered humidity changes outside the GOES areas are caused by a slightly different evolution of weather patterns between the assimilation experiment and the control. Similar humidity changes in and around the ITCZ are also found over the Atlantic when assimilating Meteosat–7 CSR. This influence of the WV radiances is consistent with the model being known to have a too static and hence too moist ITCZ. The increments caused by the geostationary WV CSR are also consistent with other radiances, as illustrated in the bottom panel: HIRS–12 observations show also higher TB than the model (corresponding to a drier/warmer upper troposphere) in the ITCZ and SPCZ. Figure 3 illustrates the potential of 4DVAR to exploit the movement of WV patterns as observed by the imagers to correct model dynamics in the upper troposphere. The left panel shows the wind

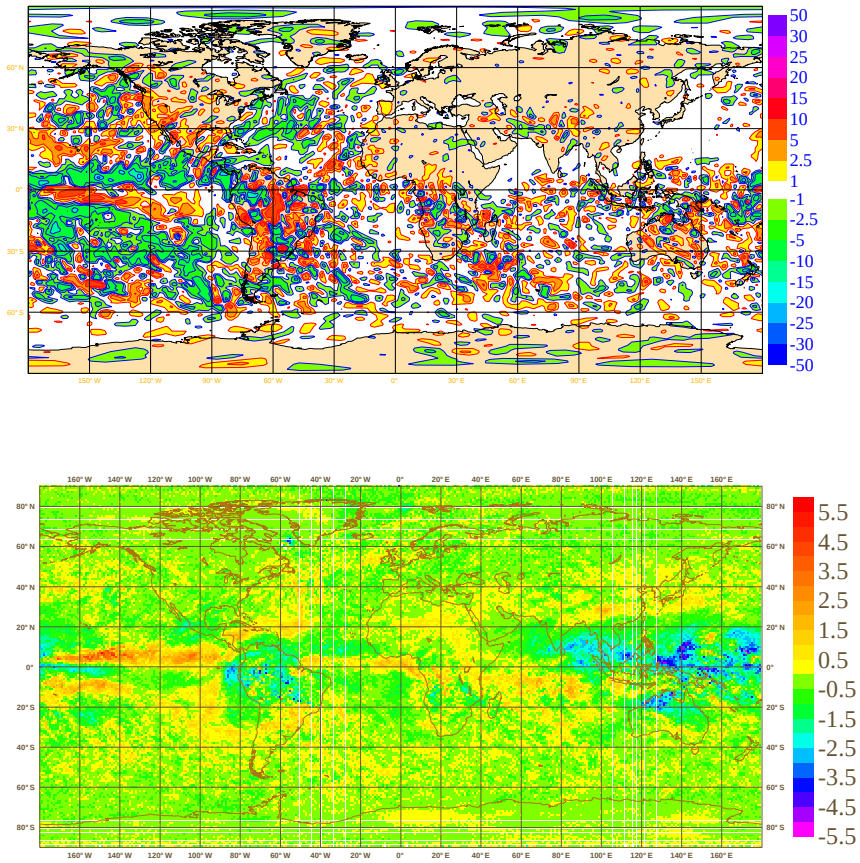

Figure 2: Top: Mean difference in analyzed relative humidity (in %) at 300 hPa between the experiment assimilating GOES WV CSR and the control. Average is from 1 February to 3 March 2002 for 00 UTC analyses. Bottom: Mean difference of HIRS channel 12 (NOAA-15, bias corrected) minus FG as brightness temperature (in K) averaged onto a 1° grid over the period 1 to 28 February 2002.

vector increments of a 4DVAR analysis of 1st April 2002 using only Meteosat-7 WV radiances, the right panel the corresponding wind field of the FG at 300 hPa. In this case, the influence of the CSR is particularly marked in the region of the trough around 25°N/18°W (west African coast) and at 15°S/10°E (central African coast) and 15°S/20°W (equatorial Atlantic). Wind increments show coherence over a deep vertical layer appropriate to the layer sounded by the WV channel. They occur primarily in the Meteosat disk area. However, especially in the jet stream areas outside the western edge of the disk, increments extend further upstream. This is linked to 4DVAR using data from the following 12 hours to correct the initial state at the beginning of this observation time window. In such a single case, the quality of the increments is difficult to assess due to insufficient observational coverage especially over the tropical and ocean areas. Statistics of obervation minus first guess differences based on longer experiments, however, show small improvement in some experiments for tropical wind observations from pilots and aircraft. This indicates a positive influence of the used sequence of WV radiances on the wind field.

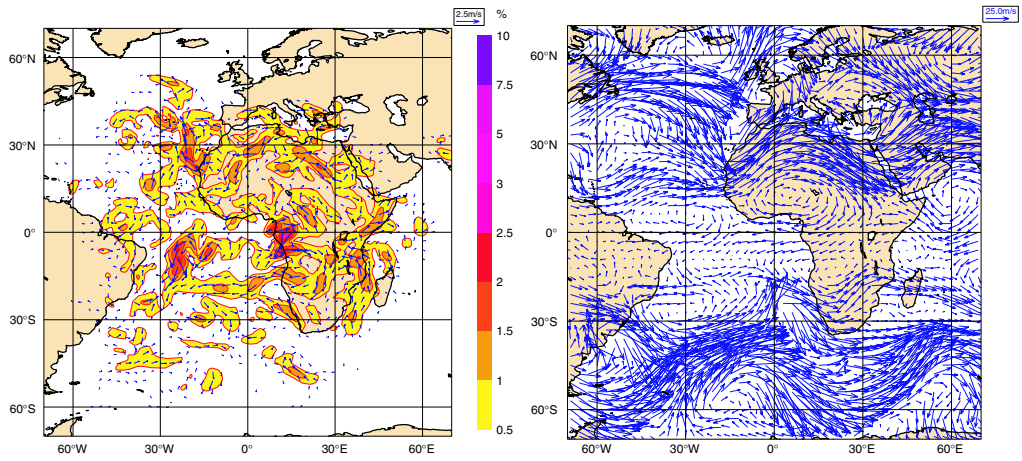

Figure 3: Left: 300h Pa wind vector increments (analysis at 3 UTC minus first guess) for 4DVAR analyis of 1st April 2002, 12 UTC using only Meteosat–7 data. The colour scale gives the wind speed in [m/s]. Right: Corresponding 300h Pa wind vector field of the first guess.

4 Assimilation verification and forecast impact

When the geostationary WV radiances are assimilated, the fit of the first guess and analysis fields to conventional observations is mostly unchanged while the first guess and analysis draw well to the geostationary CSR observations. In some experiments a slight improvement in the fit of the first guess to wind observations or radiosonde humidity can be seen. The positive impact of the WV CSR data can more clearly be seen in the fit of the model first guess to other WV radiance observations. Figure 4 shows an example of operational monitoring from a pre–operational parallel run for the period 21 February to 4 April 2002. The left page shows Meteosat–7 CSR having at least 70% clear pixels, while the right page shows statistics for HIRS–12 for data within the Meteosat–7 area and passing a window channel cloud check. The first panel on each page shows the uncorrected and the bias corrected departures from first guess and analysis, the second their standard deviation and the third the number of observations. Following a change of about 0.5 K in the Meteosat–7 bias around 26 February 2002, the CSR data were switched to passive from 4 March to 26 March in the operational test run to allow a readjustment of the Meteosat–7 bias correction. This passive period is indicated by the black curve for used data in the bottom panel dropping to zero. For Meteosat–7 radiances, spikes caused by solar stray light are visible both in the mean first guess departures and in considerably increased standard deviations of the departures (top and middle panel). After 27 March EUMETSAT exclude some severely affected slots from processing which eliminates the positive spikes (grey curve in the bottom panel giving the number of CSR observations drops to zero). However, some spurious effects remain in the distributed data as is visible in the negative spikes in the first guess departures and increased standard deviations. These affected data are not actively used in the analysis (see black curve in bottom panel giving the number of used data). With the hourly Meteosat data, the first guess error growth over the 12 hourly assimilation interval is clearly visible in the standard deviations of observation minus first guess departures. The above mentioned -0.5 K bias change of the CSR data can be seen in the bias corrected first guess departures (dotted grey curve, top panel) which drops by about -0.5 K during the days 4 to 26 March. After 26 March this is corrected through the recomputed bias correction which was based on the previous two weeks of passive processing. However, during the 6 days from 26 February to 4 March Meteosat–7 was assimilated after its bias had changed by 0.5 K but still using the previous bias correction. Since the analysis draws closely to the hourly available CSR data, the bias change is not reflected in the Meteosat–7 monitoring of observation minus first guess departures (black curve in top panel). But in the time series for the passive HIRS–12 of NOAA–16, a small change of about 0.2 K can be seen in the biases of observation minus first guess (black and grey curves in top panel on right page). The relatively small impact on the HIRS–12 bias indicates that this amount of bias uncertainty in Meteosat–7 may be tolerable, although obviously not ideal. But more importantly, the graphs demonstrate that when the Meteosat–7

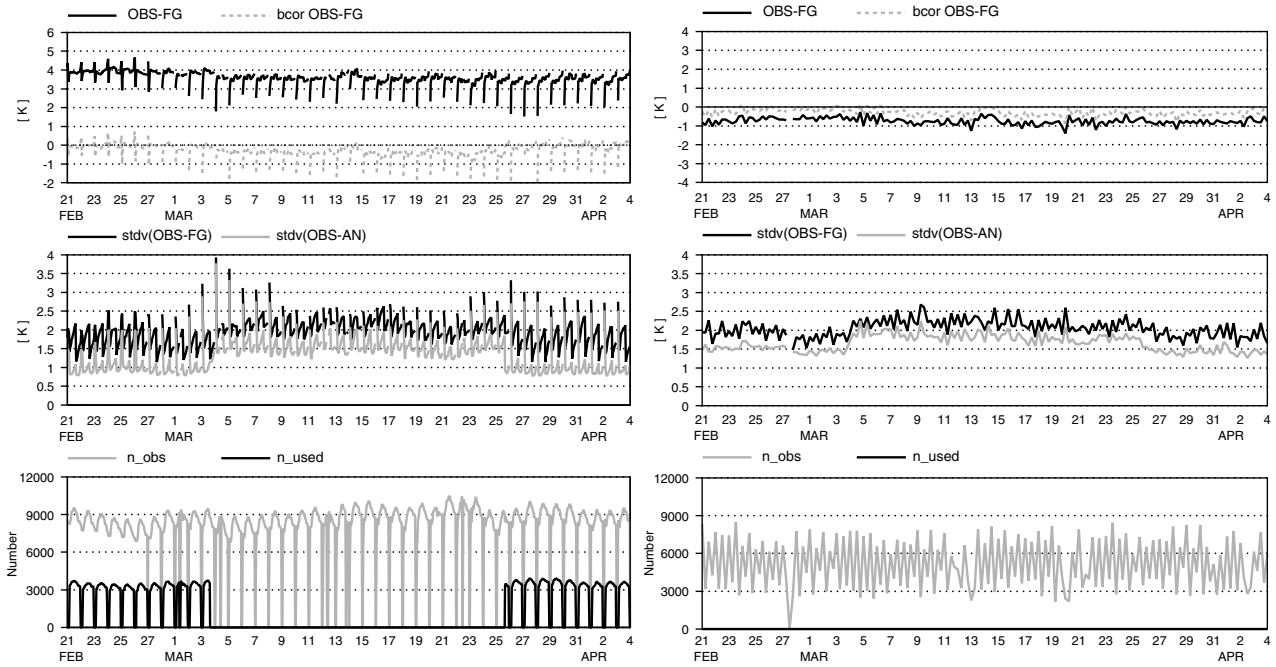

Figure 4: Time series of monitoring statistics for Meteosat–7 and HIRS–12/NOAA–16 from the pre–operational runs for the period 21 February to 4 April 2002. Statistics for Meteosat–7 (left page) use data having at least 70% clear pixels, for HIRS–12 (right page) data are from a square covering the Meteosat–7 disk. Top panel: mean observation minus first guess departure (black) and bias corrected departure (dashed grey). Second panel: standard deviation of observation minus first guess departures (black) and and observation minus analysis (grey). Bottom panel: number of data (grey) and number of used data (black).

data are not actively used in the analysis, the first guess and also the analysis fit to the radiances clearly degrade confirming the positive impact of the Meteosat–7 data in the system (see middle panels): For Meteosat–7 the standard deviations of observation minus first guess departures increases by about 0.7 K, and for HIRS–12 (as for AMSUB–3) by about 0.3-0.5 K, confirming the results from the earlier experiments.

Another test for a new data source is whether it benefits the forecast quality. This can be measured against other observations or atmospheric analyses. When measured versus observations no impact of the geostationary data could be found, but sampling in tropical areas and over the oceans is low due to sparse observations. However, when measured versus analysis fields a small, but consistently positive impact is found on geopotential and also wind fields in some areas especially at higher levels (around 200 hPa). E.g. with Meteosat–7 data a large positive impact is found over central Africa, but there is also a statistically significant reduction in the rms for the whole tropical band as illustrated in Figure 5 (left panel). Some positive forecast impact is also found in the northern extra tropical hemisphere (right panel). The small degradation in fit to analyses seen for day one is caused by the choice of the verifying analyses, being the operational analyses without the Meteosat data in this case. A verification against the analyses from the assimilation experiment results in a neutral influence on the first day. A typical impact of additional geostationary data on the forecasts of geopotential is given in Figure 6 for a four weeks assimilation experiment with GOES–8 and –10 WV CSR. For the anomaly correlation (top panels), anomaly fields of the forecast and its corresponding analysis with respect to a climatological reference field are derived and their correlation computed. There is a small but statistically significant positive impact on the southern hemisphere while for the northern hemisphere as a whole this experiment was neutral. Larger positive impact is found over the northern Pacific and northern America. Impact of Meteosat–7 data on the geopotential forecasts are of comparable magnitude. Also, the the tests with the additional HIRS data (channels 4–7, 14, and 15 and the WV channel 11 add to the operational HIRS–12) show a consistent and statistically significant positive impact of about the same magnitude, especially in the northern hemisphere.

However, it should be noted, that the magnitude of forecast impact as well as the sign of the impact in different

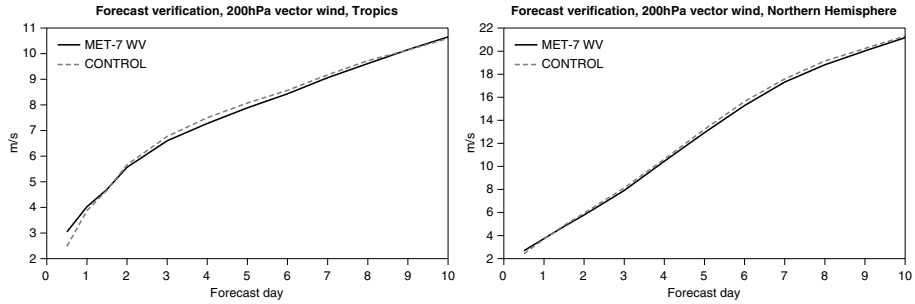

Figure 5: Root mean square error of 200 hPa winds for forecasts up to 10 days verified against operational analyses for the experiment with assimilation of Meteosat–7 WV CSR (solid line) versus the control (dashed line). Left panel is for the tropics (± 20°), right panel for the Northern hemisphere (> 20°N). The average comprises 29 cases from 2 to 30 September 2001.

areas is found to depend noticeably on the bias correction used. Similarly, a change in the bias correction used for HIRS–12 can affect the amount of impact gained from the additional geostationary radiances. Therefore, a careful tuning of the used radiances from different satellites is important.

5 Structure of humidity increments and use of revised humidity formulation

The structure of increments is determined by the observation innovation, i.e. the difference of observation minus first guess at the observation locations, and by the correlations of the model's background errors (Derber and Bouttier, 1999). Due to the high density of satellite radiances (esp. in case of geostationary CSR data), the horizontal structures reflect primarily the observation innovations and less the broder scales of the background errors. It is interesting to note that in the case of 4DVAR, some increments (in both humidity and wind fields) occur outside the disk covered by the data and expecially on the upwind side (compare Figure 3 and comments above).

An example of the vertical stucture of increments is illustrated in Figure 7 which displays a cross section through analysis increments from a 3DVAR experiment in which only Meteosat–7 data were assimilated. The increments typically occur between 100 and 700 hPa, peaking at 300 to 400 hPa. The peak and vertical extent of the increments clearly reflect the Meteosat WV channel sensitivity (weighting function). Increments from HIRS–12 data have similar vertical structures, while HIRS–11 data induce increments also lower in the atmosphere. The vertical influence due to the channel's weighting function is modulated by the first guess errors and their vertical correlation functions (based on forecast error statistics) which increases the vertical extent and shifts the peak of the increments slightly downwards. As can be seen at e.g. 39°N in the cross section, increments may even extend down to the surface despite the fact that the WV channel is not sensitive to the low levels of the atmosphere. Such increments arise from correlations in the background errors between higher and low levels. It is likely that physical parameterizations, e.g. convection, are sensitive to these increments.

The new formulation of the humidity analysis variable (Holm et al., this issue) results also in changes of the background error variances and correlation structures for the humidity variable. Therefore, the weights that observations receive under certain conditions will change as will e.g. the vertical spreading of increments. Indeed, the current operational formulation of the humidity analysis gives in certain circumstances excessive weight to the 6–micron humidity–sensitive channels like HIRS–12 and the Meteosat or GOES WV channels. This problem occurs mainly in dry subtropical air and was investigated by Andersson et al., (2000). The background error (σ_b) when expressed in terms of TB shows very marked variations over the globe. As illustrated in Figure 8 (left panel), it may reach 5–15 K in dry subtropical air. The large ratio, locally, between σ_b and σ_o (the observation errors are set to 2 K for the WV channels) results in poor conditioning of the minimisation problem

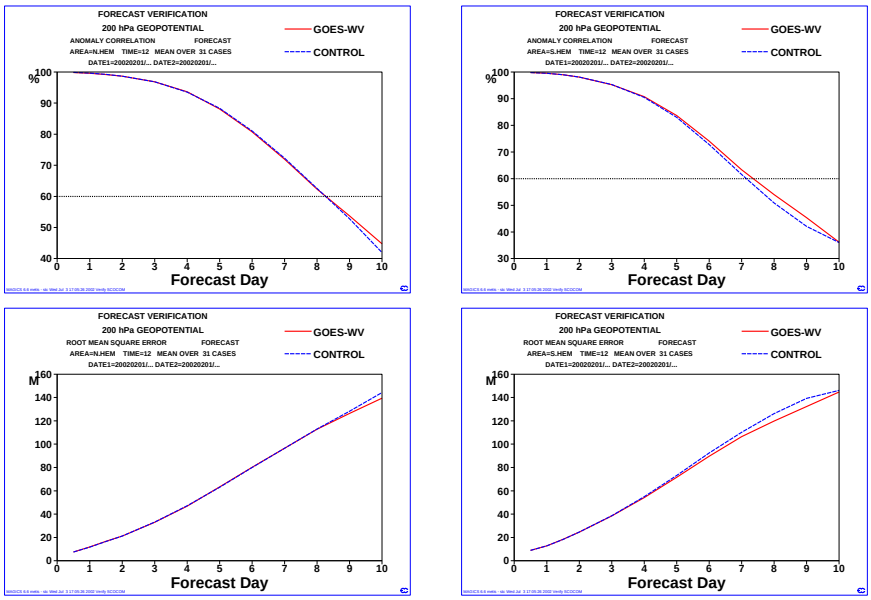

Figure 6: Anomaly correlation and root mean square error of 200 hPa geopotential for forecasts up to 10 days verified against operational analyses for the experiment with assimilation of GOES–8 and –10 WV CSR (solid line) versus the control (dashed line). Left panel is for the Northern hemisphere (> 20°N), right panel for the Southern hemisphere (< -20 °S). The average comprises 31 cases from 1 February to 3 March 2002.

and a slow rate of convergence. The large values are also in contradiction with the statistics of observation minus first guess departures which have an rms of 2.5–5 K in dry sub–tropical regions. The scatter diagram in Figure 8 shows that while for the current humidity analysis σ_b is higher than 4 K on many occasions, it hardly ever exceeds 4 K in the new formulation. Also, in dry subtropical air (high observed TB), the mean of σ_b is close to 2.5 K which is in good agreement with departure statistics, thus indicating that these data will get approximately the correct weight in the new humidity analysis.

In accordance with these changes in the background errors, the amplitude of increments is found to be diminished in many areas while the patterns (determined by the observations themselves) remain unchanged. Figure 9 illustrates this showing increments for two profiles occuring in areas of big increments in the current analysis. The two profiles are from 3DVAR analyses using Meteosat–7 data only. They show humidity increments for the current formulation (blue) and for the re–formulated (magenta) humidity analysis, respectively. The humidity increments are generally smaller with the new formulation. It should be noted that there is also less extrapolation of humidity increments to the lower troposphere due to reduced vertical background error correlations between the upper and lower levels. Often, the increment profiles tend not to be smooth but to display spikes, both in the current and the new formulations. This is caused by the σ_b depending on the value of the background value itself. E.g. the σ_b of specific humidity in the current formulation (described in Rabier et al., 1998) is small in dry conditions, so that the analysis increments at that level are strongly constrained. Also with the new formulation, the σ_b of relative humidity is smaller close to saturation or for very dry conditions (avoiding analysis increments causing unphysical relative humidities).

6 Summary and outlook

Additionally to the WV channel radiances from the polar orbiting satellites (channel HIRS–12) that have been operationally analyzed for many years, also radiances from geostationary imagers are now being used within 4DVAR to improve the analysis of upper tropospheric humidity. The radiances from the imagers are available

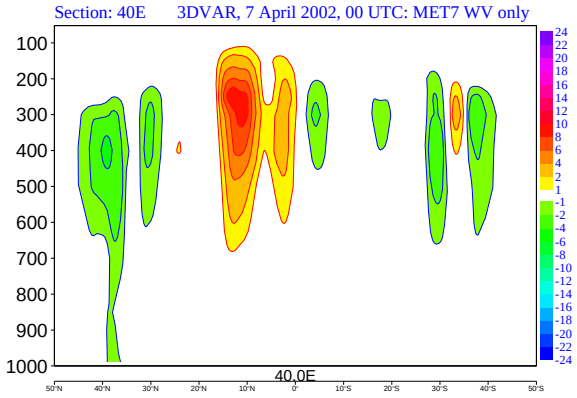

Figure 7: Vertical cross-section (versus pressure in hPa) of the relative humidity increments (analysis minus first guess, in %) at 40°E for the 3DVAR FGAT experiment for 7th April 2002, 00 UTC.

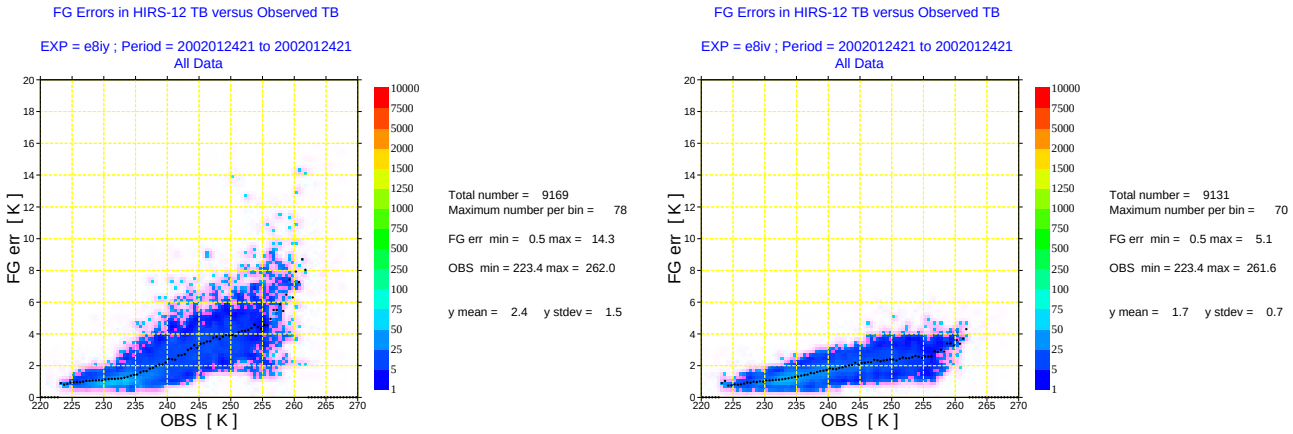

Figure 8: Background error standard deviations (in K) for Meteosat WV channel (similar to HIRS channel 12) computed using the method of Andersson et al. (2000) for the date 24 January 2002, 18 UTC for the operational (left) and the new (right) humidity analysis formulation.

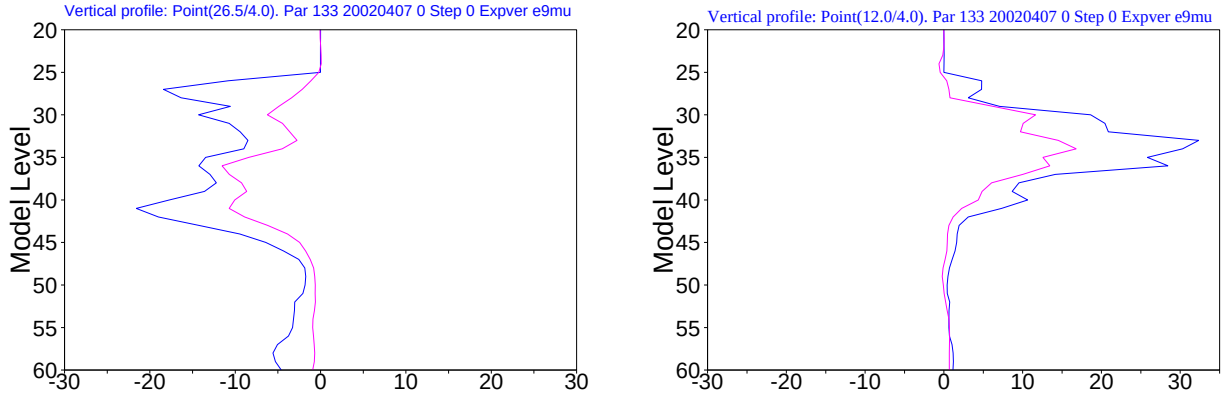

Figure 9: Two selected vertical profiles of humidity increments at a location with negative (left) and positive (right) increment from a 3DVAR analysis on 00 UTC 7 April 2002 using Meteosat–7 CSR only. The increments are expressed in percent of the background value of q for the operational (blue) and the new (magenta) formulation of the humidity analysis.

in the form of area–averaged clear–sky radiances (CSR). The CSR from Meteosat–7 have been introduced in the operational assimilation on 9 April 2002. Additional pre–operational experimentation is being carried out with CSR from both GOES-8 and GOES–10 in order to extend the geographical coverage of geostationary radiances. Extensive monitoring of the new CSR data has been carried out. Systematic biases that occur between the WV radiances of different platforms and the model first guess are diagnosed and, for assimilation purposes, removed using a statistical bias correction based on model predictors. Nevertheless (especially since the impact that the radiances have on forecast quality is found to be very sensitive to the actual bias correction applied) a more accurate calibration or calibration validation of satellite radiances would be helpful. Furthermore, the monitoring shows image anomalies caused by solar straylight intrusion for Meteosat and a 'midnight effect' in the GOES data which is possibly caused by problems in the calibration when parts of the satellite are exposed to intense heating by the sun. Data of affected time slots are excluded from assimilation and additional data selection is aimed at eliminating residual cloud contamination.

A mean impact of CSR on the moisture field is seen in areas of known model deficiencies, e.g. a high level drying of the inner ITCZ area where convection in the model tends to be too persistent. While the fit to conventional data remains unchanged, the first guess and the analysis are closer to other WV radiances showing that the WV CSR are used in the assimilation system in a consistent way. This is not only the case for other infrared radiances from HIRS–12 but also for observations in the microwave range which is particularly encouraging.

The assimilation of the hourly geostationary radiances leads also to increments in the wind field, in inner–tropical regions as well as in the jet streams. Comparisons versus conventional observations show a slightly improved fit of the first guess winds to tropical pilots in some experiments, which indicates a positive influence on the model dynamics through the use of the time sequence of radiances from geostationary orbit. This is very encouraging since data with more information content especially on the vertical atmospheric structures will become available with future (high resolution) sounders on geostationary satellites. A small, but statistically significant, positive forecast impact is seen in upper level geopotential and winds for some areas, and in some experiments for the tropics or northern hemisphere as a whole. Otherwise impact is neutral. Likewise the extension of HIRS usage to include the mid–tropospheric humidity channel 11 and the temperature channels 4–7, 14, and 15, have a small positive impact.

Experiments using the reformulation of the ECMWF humidity analysis in terms of a scaled relative humidity indicate improvements in the modelling of the model background errors and their covariances. It avoids unrealistically high weighting of the observations in very dry and warm conditions and an extrapolation of increments from the upper tropospheric WV channels to low levels. This should improve the usage made of the WV radiances in the assimilation system. Also, improved quality indicators for the CSR (being developed by the data providers) should enable further improvements in data quality control, especially with respect to remaining cloud contamination.

In future, enhanced imagers with several additional channels in the visible, infrared, and water vapor bands will become available. This ranges from the recently launched European Meteosat Second Generation (MSG) satellite to the Advanced Baseline Imager (ABI) on the GOES follow-on satellites and to the much more comprehensive measurements which can be expected from the planned advanced sounders in geostationary orbit, like the Geostationary Imaging Fourier Transform Spectrometer (GIFTS). But already in the near future, the additional visible and infrared window channels on MSG will considerably improve the cloud detection possibilities and hence the quality of CSR. Additionally, the information of two humidity sounding channels at the high time resolution of the geostationary imager will provide more vertical information useful both for the definition of the humidity fields and, in the 4DVAR context, for the indirectly derived wind increments.

Acknowledgements

This work was carried out in the framework of the EUMETSAT/ECMWF fellowship programme. This work benefited from discussions with Erik Andersson, Frédéric Chevallier and the contact persons at EUMETSAT, especially Leo van de Berg, Marie Doutriaux–Boucher, Marianne König, Rose Munro, and Stephen Tjemkes. The assistance of Rob Hine and others at ECMWF have been greatly appreciated.

References

Andersson, E., Pailleux, J., Thépaut, J.-N., Eyre, J. R., McNally, A. P., Kelly, G. A. and Courtier, P., 1994: Use of cloud-cleared radiances in three/four-dimensional variational data assimilation. *Q. J. R. Meteorol. Soc.*,**120,** 627-654.

Andersson, E., and H. Järvinen, 1999: Variational Quality control. *Q. J. Roy. Met. Soc.*, **125**, 697–722.

Andersson, E., Fisher, M., Munro, R., and McNally, A., 2000: Diagnosis of background errors for observed quantities in a variational 429 data assimilation scheme, and the explanation of a case of poor convergence. *Q. J. R. Meteorol. Soc.,* **126**, 1455–1472.

Derber, J. and F. Bouttier, 1999: A reformulation of the background error covariance in the ECMWF global data assimilation system, Tellus, **51A**, 195-222.

McNally, A. P., Derber, J. C., Wu, W. and Katz, B. B., 2000: The use of TOVS level-1b radiances in the NCEP SSI analysis system. *Q. J. R. Meteorol. Soc.*,**126,** 689-724.

Holm, E., Andersson, E., Beljaars, A., Lopez, P., Mahfouf, J-F., Simmons, A., and Thpaut, Assimilation and Modelling of the Hydrological Cycle: ECMWF's Status and Plans, *Tech. Memorandum No. 383*. Available from ECMWF, Shinfield Park, Reading, RG2 9AX, U.K.

McNally, A. P., Watts, P., D., 2002: A cloud detection algorithm for high spectral resolution infrared sounders. *Submitted to Q. J. R. Met. Soc.*

Johnson, R. X., Weinreb, M., 1996: GOES-8 imager midnight effects and slope correction. *Proceedings of SPIE conference*, 7-9 August 1996, Denver, Colorado, USA.

Köpken,C. 2001: Monitoring of METEOSAT WV radiances and Solar Stray Light Effects. *EUMETSAT/ECMWF Fellowship Report No. 10*. Available from ECMWF, Shinfield Park, Reading RG2 9AX, UK.

Köpken,C. 2002: Solar Stray Light Effects in Meteosat radiances and operational monitoring at ECMWF. *Submitted to J. Appl. Meteorol.*

Rabier, F., J.-N. Thpaut and P. Courtier, 1998: Extended assimilation forecast experiments with a four-dimensional variational assimilation system. *Q. J. R. Met. Soc.*, **124**, 1861-1887.

Köpken, C., G. Kelly, and J.-N. Thépaut, 2002: Assimilation of METEOSAT Radiance Data within the 4DVAR system at ECMWF: Part II. *Submitted to Q. J. Roy. Met. Soc.*.